

Evidence for Crossed Andreev Reflections in bilayers of (100) $YBa_2Cu_3O_{7-\delta}$ and the itinerant ferromagnet $SrRuO_3$

Itay Asulin,¹ Ofer Yuli,¹ Gad Koren,² and Oded Millo^{1,*}

¹*Racah Institute of Physics, The Hebrew University of Jerusalem, Jerusalem 91904, Israel*

²*Department of Physics, Technion - Israel Institute of Technology, Haifa 32000, Israel*

Scanning tunneling spectroscopy measurements on thin epitaxial $SrRuO_3/(100)YBa_2Cu_3O_{7-\delta}$ ferromagnet/superconductor bilayers, reveal localized regions in which the superconductor order parameter penetrates the ferromagnet to more than 26 nm, an order of magnitude larger than the coherence length in the ferromagnetic layer. These regions consist of narrow (< 10 nm) and long strips, separated by at least 200 nm, consistent with the known magnetic domain wall structure in $SrRuO_3$. We attributed this behavior to Crossed Andreev Reflections, taking place in the vicinity of the magnetic domain walls.

PACS numbers: 74.45.+c, 74.50.+r, 74.87.Bz, 74.81.-g

In spite of a considerable research effort in the past years, a comprehensive understanding of the proximity effect (PE) in superconductor (S) ferromagnet (F) heterostructures has not yet been established. Such systems are of interest since they allow a direct investigation of the interplay between the two competing orders of superconductivity and magnetism. In an N/S proximity system, where N is a normal metal in good electrical contact with S, superconducting correlations are induced in N over a length scale of the normal coherence length, ξ_N , while they are weakened in the S side over a scale of the superconducting coherence length, ξ_S ¹. The mechanism underlying the PE at S/N interfaces is the Andreev Reflection (AR). Upon impinging on the interface from the N side, hole-like quasiparticles are retro-reflected as electron-like quasiparticles with inverse spin (maintaining phase coherence over $\xi_N = \sqrt{\hbar D/k_B T}$ where D is the diffusion coefficient), while destroying Cooper pairs in the S side. Consequently, the PE is expected to be significantly suppressed when the N side is replaced by a ferromagnet due to spin polarization². Theoretical works based on the Fulde, Ferrell, Larkin and Ovchinnikov (FFLO) mechanism^{3,4}, predict a rapid and non-monotonic decay of the superconducting order parameter (OP) in F, of the form $\sin(x/\xi_F)/(x/\xi_F)$ in the clean limit and $\exp(-x/\xi_F)\cos(x/\xi_F)$ in the dirty limit (where x is the distance from the interface)^{5,6}. The corresponding coherence lengths in F where the exchange energy is E_{ex} , are $\xi_F = \hbar v_F/2E_{ex}$ (clean limit) and $\xi_F = \sqrt{(\hbar D/2E_{ex})}$ (dirty limit), which are typically of the order of a few nm, much shorter than ξ_N . For certain thicknesses of the F layer a ' π -state' may appear, in which the induced OP in F reverses its sign^{5,6}.

Many studies confirmed these predictions and clearly demonstrated damped OP oscillations in F and a corresponding dependence on the F thickness of the critical current in SFS junctions^{7,8}. All of these effects occur on a length scale of a few nm, in agreement with estimates for ξ_F . However, other experiments show a long range PE where the penetration depth of the induced order parameter in F is two orders of magnitude larger than

ξ_F ^{9,10}.

The predictions concerning the S/F proximity systems result from the singlet pairing in S, and are independent of the symmetry (s -wave or d -wave) of the order parameter^{11,12}. However, the anisotropy of the d -wave symmetry is expected to manifest itself in the PE¹¹ (as in the case of Au/YBCO bilayers we have previously studied^{13,14}), in the phase, amplitude and period of the oscillations in F. Here too, experiments provide contradictory results. While Ref. 15 reports short range damped oscillations in F, data measured on SFS Josephson junctions indicate a long range PE, sustaining for F thickness of up to 40 nm^{16,17,18,19,20}.

One possible explanation for the long range PE is given by the formation of a strong triplet pairing amplitude component^{21,22}. Alternately^{16,23}, superconducting correlations can penetrate F to a distance much longer than ξ_F in the vicinity of magnetic domain walls (DW) at the S/F interface via the Crossed Andreev Reflection (CARE) effect. This process was first discussed for two spatially separated N/S junctions²⁴, and then for three terminal S/F hybrids²⁵. Here, a spin-polarized hole arriving from one magnetic domain is Andreev reflected as an electron in an adjacent domain having opposite spin polarization. In order for CARE to occur, the width of the DW must be within a few ξ_S ^{24,25}. Peña et al.¹⁶ conjectured that CARE can explain their long range PE results in SF multilayers, in spite of the fact that the DW width in their case is $\times 10$ larger than ξ_S . Recently, evidence for CARE was provided by magnetotransport measurements performed on mesoscopic S/F structures consisting of conventional and unconventional superconductors^{26,27,28}. However, a microscopic local-probe observation of this phenomenon and its effect on the density of states (DOS) in the F side of the junctions are still lacking.

In this study we employ scanning tunneling spectroscopy on thin epitaxial $SrRuO_3/(100)YBa_2Cu_3O_{7-\delta}$ (SRO/YBCO) F/S bilayers with various SRO thicknesses. Our measurements show that the OP (induced superconductor-like gap structure) penetrates the SRO

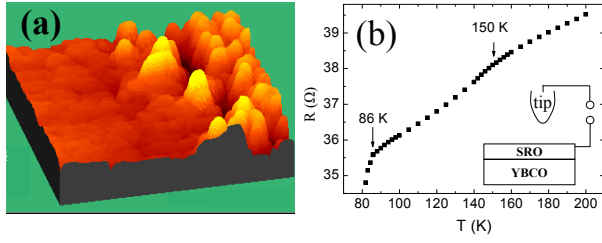


FIG. 1: (Color online) (a) 3D STM topographic image ($0.45 \times 0.45 \mu\text{m}^2$) of a 13 nm thick SRO layer on a 66 nm thick (100)YBCO film showing flat and crystalline regions typical of the bare underlying YBCO film. (b) Resistance vs. temperature curve of a 26 nm thick SRO/(100)YBCO bilayer showing both the ferromagnetic transition at ~ 150 K and the onset of the superconducting transitions at 86 K. Inset - experimental setup.

to a distance larger than $10\xi_F$ but only along well defined localized lines which correlate with the underlying magnetic DW structure. This localized long range PE may be accounted for by the CARE process taking place along the DWs of the SRO at the SRO/YBCO interface.

SRO is an itinerant ferromagnet, which is ideally suited for studying the PE with YBCO, in particular the role of the DWs. The lattice parameters of SRO are similar to those of YBCO²⁹, and therefore they can form epitaxial heterostructures with highly transparent interfaces, essential for the existence of AR and the PE. The DWs in SRO are ~ 3 nm wide, which is comparable to the YBCO coherence length of $\xi_S \sim 2$ nm, thus allowing the CARE process to occur. Marshall et al.³⁰ have shown that, depending on the growth orientation on SrTiO_3 substrates, the DW spacing varies between 200 nm and $1 \mu\text{m}$. We estimate the value of ξ_F in SRO to range between 1 nm in the dirty limit and 3 nm in the clean limit.

A total of 12 bilayers of SRO (4 to 26 nm thick) on (100)YBCO (66 nm) were prepared and measured. The (100)YBCO films were prepared by laser ablation deposition on (100) SrTiO_3 wafers in two steps. First, a 22 nm thick template layer of YBCO was deposited at a wafer temperature of 600 $^\circ\text{C}$. Then, a second 44 nm thick YBCO layer was prepared at 760 $^\circ\text{C}$. This produced films with two coexisting a-axis phases on about 95 percent of the film's area (verified by X-ray diffraction). One phase consists of small crystallites, a few unit-cells in height (~ 2 nm), while the other is composed of large areas, atomically smooth on scales of 100 nm (see Ref. 31). The bare YBCO films showed transition temperatures at around 88 K with a transition width of about 2 K, implying nearly optimally doped homogeneous films. Tunneling spectra obtained on the smooth regions of the bare YBCO sample featured 16-18 mV gaps, mainly U-shaped, further verifying the a-axis orientation³¹. The SRO layer was deposited *in-situ* on the a-axis YBCO films at 800 $^\circ\text{C}$ substrate temperature, under 100 mTorr of oxygen flow. The bilayer was then annealed in 50 Torr of oxygen for 1h at 430 $^\circ\text{C}$. Morphological features

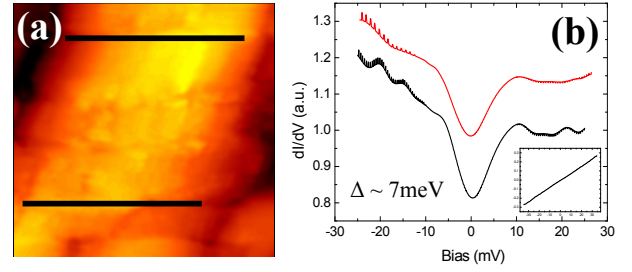


FIG. 2: (Color online) (a) $300 \times 300 \text{ nm}^2$ 2D STM image of a 9 nm thick SRO/YBCO bilayer on which an induced OP was detected along two elongated strips (marked). (b) Tunneling spectra taken, correspondingly, at the upper and lower strips marked in (a) (the upper curve is shifted vertically for clarity). Outside these gapped strips, only Ohmic I-V curves were measured (inset).

reminiscent of the flat and crystalline regions mentioned above were apparent also on the SRO-coated films. This is shown in Fig. 1a, presenting an STM image of a 13 nm thick SRO layer overcoating a (100)YBCO film. The samples were transferred from the growth chamber in a dry atmosphere and introduced into our cryogenic STM after being exposed to ambient air for less than 10 min. $R(T)$ curves of the SRO/(100)YBCO bilayers (for SRO layers thicker than 8 nm) clearly showed both the ferromagnetic transition at ~ 150 K and the superconducting transition onset around 86-90 K as seen in Fig. 1b, indicating that SRO layers at these thicknesses are still ferromagnetic but have no *pronounced* effect on the bulk superconductivity. (Zero resistance was obtained in Fig. 1b at 78 K).

The STM data presented here were all acquired at 4.2 K using a (normal metal) Pt-Ir tip as seen in the inset to Fig. 1b. The tunneling spectra were taken at specific well-defined locations correlated with the surface topography while momentarily disconnecting the feedback loop. Figure 2a presents a topographic image of a 9 nm thick (at least $3\xi_F$) SRO layer overcoating a (100)YBCO film. Within this region we observed two parallel strips, 200 nm apart (marked in black lines), along which gapped tunneling spectra were measured. Such strips will hereafter be referred to as 'gapped strips'. The dI/dV vs. V curves presented in Fig. 2b were taken correspondingly on the lower and upper gapped strips, both showing a pronounced mini-gap of $\Delta \sim 7$ mV and a normalized (with respect to the normal conductance) zero bias conductance (ZBC) of ~ 0.8 . We note that above T_c , no gaps were observed. FFLO-type PE theories^{5,6} predict that the proximity induced OP should virtually vanish for this SRO thickness ($\sim 3\xi_F$) and consequently the ZBC should be 1. Indeed the area between the two marked strips featured exclusively Ohmic (gapless) I-V curves (inset to Fig. 2b). In most cases, the location of the strips had no correlation to detectable topographic features. This excludes the possibility that the induced gap in the DOS originates from a proximity to grain boundaries, cracks

or other defects where the SRO thickness might be less than the nominal value or that ferromagnetism is locally suppressed. The distance between such ξ strips was in many cases (as in Fig. 2a) 200 nm or larger separations were also observed, consistent with the domain structure of SRO reported in Ref. 30.

A more thorough mapping of the spatial evolution of the DOS in the vicinity of such a strip is presented in Fig. 3. Figure 3b depicts a $260 \times 260 \text{ nm}^2$ topographic image of an 18 nm thick (at least $6 \xi_F$) SRO layer coating a (100) YBCO film, where the center of a ξ strip is marked by the broken blue arrow. The spectra presented in Fig. 3c were acquired sequentially at steps along this strip. Clearly, the gap in the DOS is continuous and remarkably constant *along* the strip, over the whole length that was measured (about 200 nm). Tunneling spectra depicted in Fig. 3d were taken in a similar manner *across* the strip (solid white arrow over a total length of 10 nm). Evidently, the width of the gapped area in the central region of this cross-line is less than 8 nm, comparable to the width of the DWs in (YBCO/SRO)³⁰. Within that narrow region, the gap is continuous and has a fixed width of 6.8 meV, while there are small variations. Outside this central region, the gap decays abruptly over a length of a nm and then becomes normal. (see the projection onto the x-y in Fig. 3d). We note that the gap width and ZBC vary from one strip to another on a specific film, and on average the gap structure weakens with increasing layer thickness.

Interestingly, no gapped strips were detected on films thinner than $2\xi_F$. Instead, the OP seemed to penetrate the F layer over large areas but in a non-uniform manner: for a given SRO layer thickness, gaps with a wide distribution of ZBC (0.5 to 0.85) and gap width (0.5 to 7.5 mV) were observed. The lower panel of Fig. 3 depicts two sets of dI/dV curves acquired at two different areas ($\sim 100 \times 100 \text{ nm}^2$ each) on a 6 nm thick SRO layer overcoating a (100)YBCO film. The wide distribution of the gap features cannot be solely due to SRO thickness variations. Possibly, in this low SRO thickness regime, ferromagnetism might be weakened in parts of the F layer and the domain structure may be lost. Indeed, the kink seen at 150 K in the $R(T)$ curve of Fig. 1b could hardly be observed on these bilayers. The upper panel of Fig. 4 depicts a typical dI/dV curve obtained on an area adjacent to the area where the small gap curves below it were measured. This curve shows a peak in the DOS at zero bias, the shape and size of which (compared to the curves plotted below it) are consistent with the formation of a π -state.

We believe that the origin for the observed localized and long-range ($\geq 10\xi_F$) penetration depth of the OP into the SRO layer is the CARE process, taking place along the DWs at the SRO/YBCO interface (see Fig. 3a). Consequently, superconducting correlations can penetrate F quite efficiently in the vicinity of a DW. Naively speaking, Cooper pairs are injected into the F

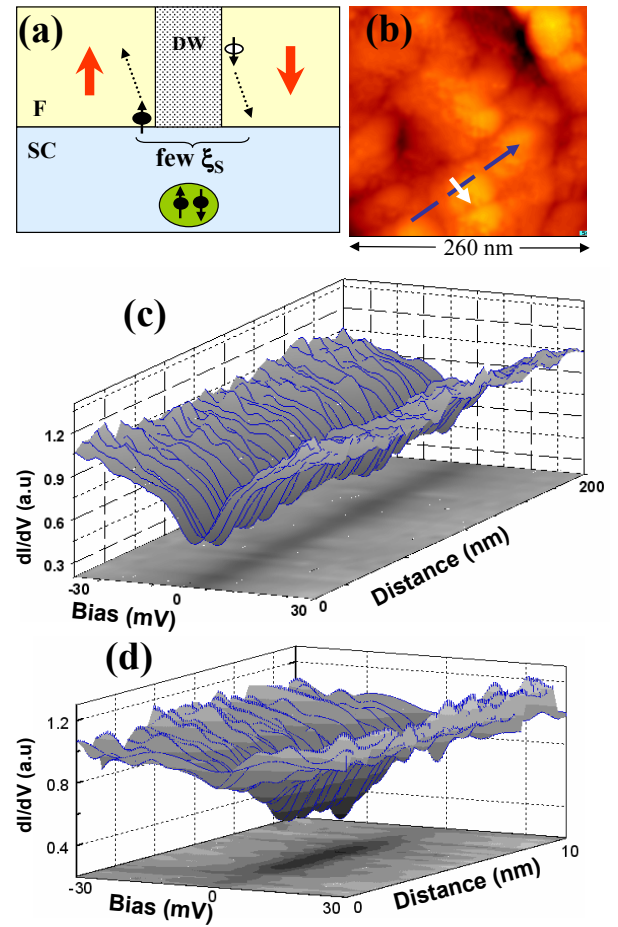


FIG. 3: (Color online) STM measurement demonstrating the spatial evolution of the DOS within a 'gapped strip' in the SRO. (a) A schematic CARE diagram. (b) $260 \times 260 \text{ nm}^2$ topographic image of a 18 nm thick SRO/(100)YBCO bilayer. (c) Tunneling spectra taken sequentially at fixed steps along the center of the gapped strip (marked by the blue arrow in (b)). (d) Tunneling spectra acquired across the gapped strip (solid white arrow in (b)).

layer and can diffuse deeper inside only along a DW up to distances comparable to those of the PE in the S/N case¹³. Recall that the DW width is comparable to ξ_S and much smaller than the phase coherence length ($\sim \xi_N$) at 4.2 K, thus the conditions required for the local long range PE are satisfied. The narrow width and the spacing of the elongated gapped strips in our measurements are in agreement with the known configuration and size of the DWs in SRO³⁰. Our results support the recent magneto-transport evidence for CARE in YBCO/SRO/YBCO junctions with similar SRO layer thicknesses²⁸, and corroborate the prediction that the total Andreev conductance of an S/F interface is proportional to the total length of the DWs crossing it³². The triplet pairing scenario for the long range PE is unlikely in our case since it would have resulted in a penetration of the OP *all over* the SRO layer. However, we cannot

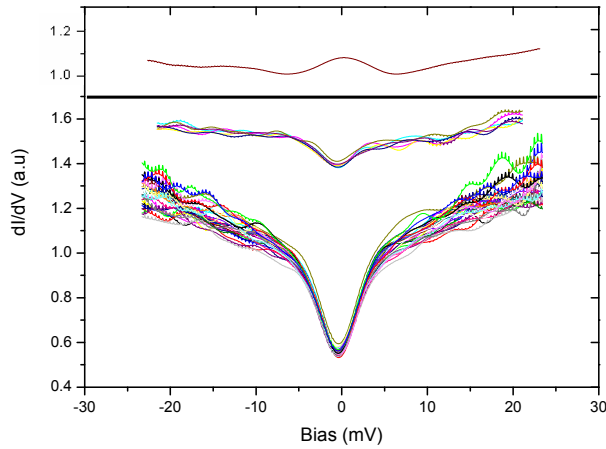


FIG. 4: (Color online) Lower panel: two sets of tunneling spectra taken at different areas ($100 \times 100 \text{ nm}^2$ each) on a 6 nm thick SRO/(100)YBCO bilayer. Gap size and ZBC corresponding to the upper and lower sets are: 3.8 mV, 0.85 and 4.5 mV, 0.56, respectively. Upper panel: a dI/dV curve showing a peak at zero bias, possibly manifesting a π -state.

exclude the possibility that the long range PE may be due to the reduced spin polarization inside the DWs that may locally enhance the conventional AR.

We suggest that the CARE process may also account for the results reported by Gausepoh et. al.¹⁷ and Dömel

et al.¹⁹. In both cases, supercurrents were observed in YBCO/SRO/YBCO ramp junctions with 20 nm thick SRO barriers. In the former, nonuniformity in the supercurrent density over the area of the junctions was inferred from the magnetic response and related to the existence of favorable interface regions, less than 10 nm wide, through which the supercurrent flows. In the latter, the results were attributed to resonant tunneling through localized states. Our data imply that the localized behavior in both cases may possibly be an effect of the existence of DWs in the SRO layer through which the superconducting electrodes couple. In the opposite case, where no DWs are present at an F/S interface, the 'conventional' short range PE is expected to take place, as was recently demonstrated experimentally³³.

In summary, we found a remarkably localized and long ranged PE in bilayers of SRO on (100)YBCO. For SRO layers thicker than $\sim 3\xi_F$, the OP penetrates the SRO to a distance larger than $10\xi_F$ only along well defined localized lines which correlate with the underlying magnetic DW structure. This localized long range PE is thus attributed to the CARE process taking place along the DWs of the SRO layer.

The authors are grateful to G. Deutscher, and L. Klein, for useful discussions. This research was supported in part by the Israel Science Foundation, Center of Excellence program (grant # 1564/04).

-
- * Electronic address: milode@vms.huji.ac.il
- ¹ G. Deutscher and P. G. De Gennes, *Superconductivity* (Marcel Dekker, Inc., New York, 1969).
 - ² R. J. Soulen et al., *Science* **282**, 85 (1998).
 - ³ P. Fulde, and R. A. Ferrell, *Phys. Rev.* **135**, A550 (1964).
 - ⁴ A. Larkin, and Y. Ovchinnikov, *Sov. Phys. JETP* **20**, 762 (1965).
 - ⁵ E. A. Demler, G. B. Arnold, and M. R. Beasley, *Phys. Rev. B* **55**, 15174 (1997).
 - ⁶ A. Buzdin, *Rev. Mod. Phys.* **77**, 935 (2005).
 - ⁷ T. Kontos et al., *Phys. Rev. Lett.* **86**, 304 (2001).
 - ⁸ V. V. Ryazanov et al., *Phys. Rev. Lett.* **86**, 2427 (2001).
 - ⁹ M. Giroud et al., *Phys. Rev. B* **58**, R11872 (1998).
 - ¹⁰ V. T. Petrashov et al., *Phys. Rev. Lett.* **83**, 3281 (1999).
 - ¹¹ Z. Faraii and M. Zareyan, *Phys. Rev. B* **69**, 014508 (2004).
 - ¹² N. Stefanakis and R. Mélin, *J. Phys: Condensed Matter* **15**, 3401 (2003).
 - ¹³ A. Sharoni et al., *Phys. Rev. Lett.* **92**, 017003 (2004).
 - ¹⁴ I. Asulin et al., *Phys. Rev. Lett.* **93**, 157001 (2004).
 - ¹⁵ M. Freamat and K. W. Ng, *Phys. Rev. B* **68**, 060507(R) (2003).
 - ¹⁶ V. Peña et al., *Phys. Rev. B* **69**, 224502 (2004).
 - ¹⁷ S. C. Gausepohl, et. al., *Appl. Phys. Lett.* **67**, 1313 (1995).
 - ¹⁸ L. Antognazza et al., *Appl. Phys. Lett.* **63**, 1005 (1993).

- ¹⁹ R. Dömel et al., *Appl. Phys. Lett.* **67**, 1775 (1995).
- ²⁰ R. Dömel et al., *Supercond. Sci. Technol.* **7**, 277 (1994).
- ²¹ F. S. Bergeret, A. F. Volkov, and K. B. Efetov, *Phys. Rev. Lett.* **86**, 4096 (2001).
- ²² A. F. Volkov, F. S. Bergeret, and K. B. Efetov, *Phys. Rev. Lett.* **90**, 117006 (2003).
- ²³ T. Heikkilä, Doctoral Dissertation, Helsinki University of Technology, 2002.
- ²⁴ J. M. Byers and M. E. Flatté, *Phys. Rev. Lett.* **74**, 306 (1995).
- ²⁵ G. Deutscher and D. Feinberg, *Appl. Phys. Lett.* **76**, 487 (2000).
- ²⁶ D. Beckmann, H. B. Weber, and H. v. Löhneysen, *Phys. Rev. Lett.* **93**, 197003 (2004).
- ²⁷ M. Giroud et al., *Eur. Phys. J. B* **31**, 103 (2003).
- ²⁸ P. Aronov, and G. Koren, *Phys. Rev. B* **72**, 184515 (2005).
- ²⁹ N. D. Zakharov et al., *J. Mater. Res.* **14**, 4385 (1999).
- ³⁰ A. F. Marshall et al., *J. Appl. Phys.* **85**, 4131 (1999).
- ³¹ A. Sharoni et al., *Europhys. Lett.*, **62**, 883 (2003).
- ³² N. M. Chitchev and I. S. Burmistrov, *Phys. Rev. B* **68**, 140501(R) (2003).
- ³³ J. Aumentado and V. Chandrasekhar, *Phys. Rev. B* **64**, 054505 (2001).